Determination of the Structures of Antiinflammatory Copper(II) Dimers of Indomethacin by Multiple-Scattering Analyses of X-ray Absorption Fine Structure Data

Jane E. Weder,[†] Trevor W. Hambley,*[,†] Brendan J. Kennedy,*[,†] Peter A. Lay,*[,†] Garry J. Foran,[‡] and Anne M. Rich[†]

Centre for Heavy Metals Research, School of Chemistry, University of Sydney, Sydney, NSW 2006 Australia, and Australian Nuclear Science and Technology Organisation (ANSTO), PMB 1 Menai, NSW 2234 Australia

Received July 14, 2000

Copper K-edge X-ray absorption spectroscopic (XAS) measurements were recorded for the veterinary antiinflammatory Cu(II) complexes of indomethacin (1-(4-chlorobenzoyl)-5-methoxy-2-methyl-1H-indole-3-acetic acid = IndoH), of the general formula $[Cu_2(Indo)_4L_2]$ (L = *N*,*N*-dimethylformamide (DMF), *N*,*N*-dimethylacetamide (DMA), *N*-methylpyrrolidone (NMP), and water), and $[Cu_2(OAc)_4(OH_2)_2]$ at room temperature and 10 K. The bond lengths and bridging O−C−O angles of the dimeric Cu(II) cage ($Cu_2O_{10}C_8$) obtained from the multiple-scattering (MS) fitting of the X-ray absorption fine structure (XAFS) using a centrosymmetric model of $[Cu_2(Indo)_4(DMF)_2]$ gave Cu···Cu = 2.62(2) Å, mean $Cu-O_{Ac}$ = 1.95(2) Å, $Cu-O_L$ = 2.15(2) Å, bridging O−C−O = 125(1)°, Cu displacement from plane 0.19 Å compared with the XRD data Cu···Cu = 2.630(1) Å, mean $Cu-O_{Ac}$ = 1.959 Å, $Cu-O_L$ = 2.143(5) Å, bridging O−C−O angles = 123.2(5)°, Cu displacement from plane 0.20 Å. The excellent agreement between the XAFS- and XRD-derived data allowed the structures of related $[Cu_2(Indo)_4L_2]$ (L = DMA, NMP) complexes to be determined. All display a similar $Cu_2O_{10}C_8$ coordination geometry, which is independent of the nature of the axial ligand. While XAFS analysis of $[Cu_2(Indo)_4(OH_2)_2]$ and $[Cu_2(OAc)_4(OH_2)_2]$ indicates a coordination geometry similar to that of $[Cu_2(Indo)_4L_2]$ (L = DMF, DMA, NMP), removal of symmetry restraints in the MS model is required to obtain axial bond lengths comparable to those derived in the XRD structures of the acetate complex. For the Indo complex, the fitted bond lengths with the lower symmetry model give a mean $Cu-L_{OH_2}$ bond distance within experimental errors of the value for $[Cu_2(Indo)_4(DMSO)_2]$ (2.16(2) Å) (XRD). The difficulty in refining the $Cu-O_{(OH_2)}$ distance of $[Cu_2(OAc)_4(OH_2)_2]$ and $[Cu_2(Indo)_4(OH_2)_2]$ using a centrosymmetric MS model is attributed to a symmetry reduction due to hydrogen-bonding effects characteristic of the aqua adducts, as is observed in the XRD structure of the acetate complex.

Introduction

Indomethacin (1-(4-chlorobenzoyl)-5-methoxy-2-methyl-1H-indole-3-acetic acid = IndoH) (**1**) is one of the most potent of the

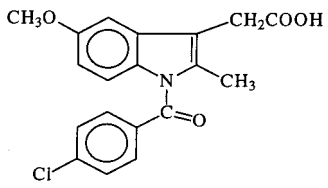

1

clinically used nonsteroidal antiinflammatory drugs (NSAIDs).[1,2] Adverse gastrointestinal (GI) side effects related to the inhibition of prostaglandin synthesis[3,4] limits the dose and more widespread use of the NSAIDs.[1,2,5,6] Despite these problems, IndoH is used clinically in the treatment of acute inflammation[1,2,7] and other specialized medical conditions[8,9] in humans. The severity of the GI toxicities of IndoH is highlighted by the drug's contraindication in dogs due to fatal GI ulceration and hemorrhage,[10−12] whereas the Cu(II) complex of the NSAID can be safely administered.[13] The need to develop potent, yet less GI irritating, NSAIDs has led to several studies on the preparation, characterization, and medical use of M(II) complexes of IndoH and other NSAIDs,[14−18] most importantly the Cu(II) complexes of IndoH. There are suggestions that Cu(II) may play a role in

[†] University of Sydney.
[‡] Australian Nuclear Science and Technology Organisation (ANSTO).

(1) Thomas, J. *Australian Prescription Products Guide*, 26th ed.; Australian Pharmaceutical Publishing Co. Ltd.: Hawthorn, Victoria, 1997; Vol. 1, p 1327−1336.
(2) Reynolds, J. E. F. *Martindale. The Extra Pharmacopoeia*, 31st ed.; The Pharmaceutical Press: London, 1996.
(3) Dukes, M. N. G. *Meyler's Side Effects of Drugs. An Encyclopedia of Adverse Reactions and Interactions*, 13th ed.; Elsevier: Amsterdam, 1996.
(4) Abramson, S. B.; Weissmann, G. *Arthritis Rheum.* **1989**, *32*, 1−9.
(5) Goodman, L. S.; Gilman, A. *The Pharmacological Basis of Therapeutics*, 5th ed.; Macmillan Publishing Co., Inc.: New York, 1975.
(6) Armstrong, C. P.; Blower, A. L. *Gut* **1987**, *28*, 527−532.
(7) Goes, F.; Trinquand, C. *B. Soc. Belg. Oph.* **1997**, *267*, 11−19.
(8) Mosca, F.; Bray, M.; Lattanzio, M.; Fumagalli, M.; Toestto, C. *J. Pediatr.* **1997**, *131*, 549−554.
(9) Sterniste, W.; Gabriel, C.; Sacher, M. *Pediatr. Card.* **1998**, *19*, 256−258.
(10) Adams, H. R., Ed. *Veterinary Pharmacology and Therapeutics*, 7th ed.; Iowa State University Press: Ames, IA, 1995; pp 443−444.
(11) Menguy, R.; Desbaillets, L. *Am. J. Dig. Dis.* **1967**, *12*, 862−866.
(12) Ewing, G. O. *J. Am. Vet. Med. Assoc.* **1972**, *161*, 1665−1668.
(13) *IVS Annual*; MIMS Publishing: Crows Nest, N.S.W., Sydney, 1997; pp 145, 276.
(14) Sorenson, J. R. J. *Inflammatory Diseases and Copper*, 1st ed.; Humana Press: Clifton, NJ, 1982.
(15) Auer, D. E. Ph.D. Thesis, University of Queensland, Queensland, Australia, 1987.

10.1021/ic0007815 CCC: $20.00
Published on Web 02/13/2001

preventing the GI damage associated with use of some NSAIDs.[14,19] Furthermore, Cu(II) NSAIDs display more potent antiinflammatory action than either the parent NSAID or uncomplexed Cu(II), with the additional benefit of antiulcerogenic activity.[14,20]

Copper complexes of IndoH are increasingly used as veterinary pharmaceutics[13] with ~12 million doses of $[Cu_2(Indo)_4(DMF)_2]$ having been safely administered to dogs.[21] However, their chemical and physical properties, including their structures, need to be understood for their potential as potent, yet safer, human antiinflammatory drugs to be explored. Diffraction quality crystals of Cu(II) complexes of IndoH are difficult to prepare, and to date, only crystal structures of $[Cu_2(Indo)_4L_2]$ (L = DMF or DMSO) have been reported.[16,17] These two Cu(II) complexes of IndoH exhibit a dimeric structure similar to that of $[Cu_2(OAc)_4(OH_2)_2]$,[22−24] with a $Cu_2O_{10}C_8$ core and a Cu···Cu separation of 2.61−2.63 Å.[16,17] EPR spectroscopic studies of powdered $[Cu_2(Indo)_4L_2]$ (L = DMF, DMA, NMP, OH_2) demonstrate that a dimeric structure was retained irrespective of the axial ligand, although a varying amount of monomeric species (less than 9%) is also present.[17] Structural characterization of Cu(II) complexes of IndoH in pharmaceutical preparations and biological samples is equally important; hence, multiple-scattering (MS) analysis of X-ray absorption fine structure (XAFS) has been explored as a generally applicable method of such characterization. Previously, single-scattering (SS) XAFS analyses of Cu(II) complexes with a variety of dinucleating ligands involving carboxylates,[25] sulfides and benzimidazoles,[26] and metallothioneins have been used to determine their coordination geometries.[27] However, SS analysis provides no information on the spatial arrangements of the atoms around the absorbing metal center, whereas MS analysis does.[28,29]

Caution has been recommended in accepting unexpectedly long XAFS-fitted $Cu-O_L$ distances obtained from SS analyses of dimers.[30] For instance, the SS analysis of $[Cu_2(OAc)_4(OH_2)_2]$ in liquid and glassy states gave $Cu-O_L$ bond distances that are longer (2.28−2.37 Å)[31] than that determined from XRD data (2.156(4) Å).[24] To test the ability of modern XAFS techniques to accurately model the $Cu_2O_{10}C_8$ core in dimeric Cu(II) complexes with bridging alkanoate oxygens, microcrystalline powders of crystallographically characterized $[Cu_2(Indo)_4(DMF)_2]$ and $[Cu_2(OAc)_4(OH_2)_2]$ have been studied at room temperature (RT) and/or 10 K. Also reported are the applications of MS analysis of XAFS of microcrystalline $[Cu_2(Indo)_4L_2]$ (L = DMA, NMP, OH_2) that have not been structurally characterized, to examine any changes in the $Cu_2O_{10}C_8$ coordination geometry as a result of changes in the axial ligand.

Experimental Section

Synthesis. Indomethacin was of pharmaceutical grade (Sigma Pharmaceuticals). $[Cu_2(OAc)_4(OH_2)_2]$ was obtained from Univar (99% purity). All other chemicals were of analytical grade (Aldrich or Sigma). These were used without further purification. The $[Cu_2(Indo)_4L_2]$ (L = DMF, DMA, NMP) complexes were synthesized as reported previously.[17] The Cu(II) complexes were protected against light and moisture during storage. An aqua complex of IndoH was also prepared as for $[Cu_2(Indo)_4L_2]$ (L = DMF, DMA, NMP) except that MeCN was used as the solvent, resulting in $[Cu_2(Indo)_4(OH_2)_2]\cdot 1.5H_2O$. Anal. ($Cu_2C_{76}H_{69}Cl_4N_4O_{20.5}$) C, H, N, Cu: calcd, 56.4, 4.2, 3.5, 7.9; found, 56.1. 4.2, 3.3, 8.0.

Thermogravimetric Analysis (TGA). Dynamic TGA of the aqua adducts of the Cu(II) IndoH complexes were conducted with a TA instruments HI-Res TGA 2950 thermogravimetric analyzer equipped with a Platinel II thermocouple. A constant heating rate of 20 °C min^{-1} was used from RT to 800 °C, and the weight loss of the samples was recorded every 2 s.

XAS Sample Preparation and Data Collection. Samples for XAS measurements were ground to a fine powder and used without further dilution (~7.5 wt % Cu). The powders were pressed into an Al sample holder (~1.0 mm thick) and secured with Kapton tape windows. The low-temperature samples were prechilled in liquid nitrogen prior to insertion into a Crydone REF-1577-D22 closed-cycle cryostat, and samples were maintained at 10 K with a Neocera LTC-11 temperature controller unit.

The Cu K-edge XAS was measured (Table S1 of Supporting Information) at the Australian National Beamline Facility (ANBF) on bending magnet beamline 20B at the KEK Photon Factory, Tsukuba Synchrotron Radiation Laboratory, Tsukuba, Japan, using a Si(111) channel-cut monochromator. The storage ring delivered a current of 250−400 mA at 2.5 GeV. Three scans of the X-ray absorption spectrum were recorded in transmission mode at RT and 10 K using standard N_2-filled ionization chambers. The monochromator crystal was detuned 50% throughout the Cu K-edge XAFS measurements to reduce the harmonic interference. Energies were calibrated with a Cu foil, the first inflection point being assigned as 8980.3 eV.[32] The scans were averaged using weights based on the signal-to-noise ratios, with each XAFS spectrum checked individually before averaging, and any monochromator glitches were removed. A background correction was applied by fitting a single-segment second-order polynomial spline curve to the preedge region, extrapolating it into the XAFS region, and subtracting it from the data. A three-region, second-order spline was fitted to the XAFS region at approximately 9021, 9225, 9669, and 10 127 eV and subtracted. The data were normalized to an edge jump of 1.0, where the edge jump denotes the underlying intensity of the Cu edge after subtracting the XAFS, and compensated for decreasing absorbance past the edge. The background-subtracted, normalized, and compensated data were converted to k^3 space, where k is the photoelectron wave vector, to enhance the amplitude of the high k oscillations.

XFIT Data Analysis. SS and MS analyses of XAFS data were performed using the XFIT program, which employs nonlinear least-squares fitting to vary the model until the agreement between the

(16) Weser, U.; Sellinger, K. H.; Lengfelder, E.; Werner, W.; Strahle, J. *Biochim. Biophys. Acta* **1980**, *631*, 232−245.
(17) Weder, J. E.; Hambley, T. W.; Kennedy, B. J.; Lay, P. A.; MacLachlan, D.; Bramley, R.; Delfs, C. D.; Murray, K. S.; Moubaraki, B.; Warwick, B.; Biffin, J. R.; Regtop, H. L. *Inorg. Chem.* **1999**, *38*, 1736−1744.
(18) Regtop, H. L.; Biffin, J. R. Australia Patent 89-4328 890522 and U.S. Patent 92-773601920115 (Divalent Metal Salts of Indomethacin as Antiinflammatory and Analgesic Agents), 1990.
(19) Boyle, E.; Freeman, P. C.; Goudie, A. C.; Mangan, F. R.; Thomson, M. *J. Pharm. Pharmacol.* **1976**, *28*, 865−868.
(20) Sorenson, J. R. J. In *Copper and Zinc in Inflammation*; Milanino, R., Rainsford, K. D., Velo, G. P., Eds.; Kluwer Academic Publishers: Dordrecht, 1989; pp 69−84.
(21) Biffin, J. R. Safe Administration of Copper Indomethacin in Australia to Dogs. Personal communication (Biochemical Veterinary Research, P.O. 755, Mittagong, N.S.W., 2575, Australia), 2000.
(22) Bleaney, B.; Bowers, K. *Proc. R. Soc. London., Ser. A* **1952**, 451−465.
(23) van Niekerk, J. N.; Schoening, F. R. L. *Acta Crystallogr.* **1953**, *6*, 227−232.
(24) de Meester, P.; Fletcher, S. R.; Skapski, A. C. *J. Chem. Soc., Dalton Trans.* **1973**, 2575−2578.
(25) Sarode, P. R.; Sankar, G.; Rao, C. N. *Proc. Ind. Acad. Sci. (Chem. Sci.)* **1983**, *92*, 527−542.
(26) Benzekri, A.; Cartier, C.; Latour, J.; Limosin, D.; Rey, P.; Verdaguer, M. *Inorg. Chim. Acta* **1996**, *252*, 413−420.
(27) Abrahams, I. L.; Bremner, I.; Diakun, G. P.; Garner, C. D.; Hasnain, S. S.; Ross, I.; Vasak, M. *Biochem. J.* **1986**, *236*, 585−589.
(28) Gurman, S. J. *J. Synchrotron Radiat.* **1995**, *2*, 56−63.
(29) Riggs-Gelasco, P. J.; Stemmler, T. L.; Penner-Hahn, J. E. *Coord. Chem. Rev.* **1995**, *144*, 245−286.
(30) Hathaway, B. J. In *Comprehensive Coordination Chemistry. The Synthesis, Reaction, Properties & Application of Coordination Compounds*; Wilkinson, G., Gillard, R. D., McCleverty, J. A., Eds.; Pergamon Press: Oxford, 1987; Vol. 5, pp 634−774.
(31) Nomura, M.; Yamaguchi, T. *J. Phys.* **1986**, *C8* (Suppl. 12), 619−622.
(32) George, G. N. *Centre for X-Ray Optics X-Ray Data Booklet*; SSRL: Berkeley, CA, 1993.

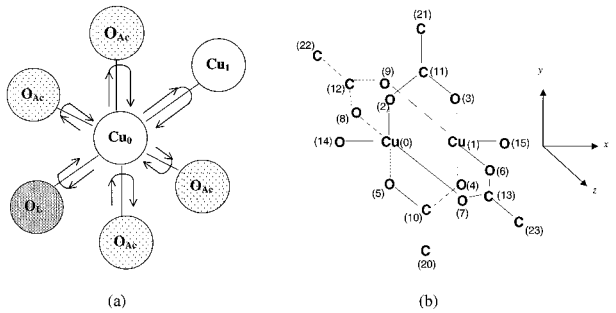

Figure 1. (a) Three-shell (1Cu + 4Cu−O_{Ac} + 1Cu−O_L) SS model. (b) MS XAFS model for the [Cu_2(Indo)$_4L_2$] (L = DMF, DMA, NMP, OH_2) core.

observed and calculated XAFS was optimized.[33] The goodness of fit parameter (R_{xaf}) was calculated as[34]

$$R_{xaf} = \left[\frac{\sum(k^3(\text{data} - \text{fit}))^2}{\sum(k^3(\text{data}))^2}\right]^{1/2} \quad (1)$$

where an R_{xaf} value around 20% is considered a good fit to non-Fourier transformed data, while an R_{xaf} value greater than 40% is poor.[35]

Ab initio phase and amplitude parameters were calculated using the SS FEFF 4.06 program and the curved-wave MS program FEFF 6.01.[36−38] Both the observed and calculated XAFS and Fourier transform (FT) data were filtered. The XAFS (k space) and FT (r space) window parameters were typically set at 0−12.4 Å^{-1} and 0.7−4.6 Å and at 0−12.4 Å^{-1} and 0.7−2.4 Å for the MS and SS analyses, respectively. The k and r windows used for the XAFS analyses are shown in the XAFS and FT figures, respectively. The parameters treated as variables in order to optimize the agreement between the observed and calculated XAFS were the positional parameters (x, y, z) of the atoms in the model, the Debye−Waller factors σ^2, the scale factor S_o^2, and the threshold energy E_o.

Statistical errors in bond distances and bond lengths due to noise in the XAFS data were determined by Monte Carlo calculations.[33,39] Typical systematic errors (σ_s) in the metal−nitrogen/oxygen distances in XAFS analysis of 0.01−0.02 Å [28] were combined with the Monte Carlo calculations of statistical errors (σ_r)[33] to obtain the estimated maximum root-mean-square (rms) error ($[\sigma_r^2 + \sigma_s^2]^{1/2}$).[40] The value of σ_s for the bridging O−C−O bond angle was calculated using the esd's of the O···O and O−C bond distances. Typically, systematic errors in bond angles of 1° were calculated for bond lengths with an esd of 0.02 Å. The estimated maximum rms errors are shown in this work as standard deviations in the reported bond distances and angles.

SS and MS Fits to the XAFS Models. All models were based on the crystal structure of [Cu_2(Indo)$_4$(DMF)$_2$]·1.6DMF (Table S2 and Figure S1 of Supporting Information) for the starting distances and angles.[17] A two-shell SS model (1Cu + 5O) and the three-shell model (1Cu + 4O_{Ac} + 1O_L) (Figure 1) were used to examine whether the two oxygen shells could be distinguished by SS analysis. A seven-shell SS model (Table S3 of Supporting Information) of the XAFS of [Cu_2(Indo)$_4$(DMF)$_2$] at 10 K was investigated for comparison with the results of the MS fitting of the XAFS.

The starting centrosymmetric MS XAFS model consists of Cu···Cu and Cu−O_L vectors along the x axis in addition to the four carboxylate carbons of the $Cu_2O_{10}C_8$ core (N = 10, 11, 12 and 13) at 2.84 Å in distance from Cu_0 on the y and z axes, respectively (Figure 1). The β-carbon atom of each of the four Indo moieties (N = 20, 21, 22 and 23) was started at ∼4.2 Å from Cu_0. A center of symmetry was located at the origin of the model (corresponding to the midpoint of the Cu···Cu vector). The MS XAFS model bond angle (deg) and bond length (Å) restraints, Debye−Waller restraints (σ^2 (Å^2)), and positional parameter (x, y, z) constraints are given in the Supporting Information. Starting Cu−O_L vector distances in the range 2.00−2.17 Å were investigated.

All Debye−Waller factors were restrained to be greater than zero (σ > 0.001(0.0005) (Å^2)) and less than 0.08 (σ < 0.08(0.001) (Å^2)) (Table S4 of Supporting Information). The Debye−Waller factors were set to increase in value with increasing distance from the Cu absorber, with identical shells constrained to be equal. The incorporation of constraints and restraints was used to reduce the degrees of freedom in the model and hence result in faster convergence of the refinements (Table 1 and Tables S5 and S6 of Supporting Information) and improved determinacy of the model.[35] While an increase in the value of the XAFS weighting factor from 1 to 8 results in a decrease in the value of R_{xaf} for [Cu_2(Indo)$_4L_2$] (L = DMF, OH_2) (10 K) (Table S6), the difference between the expected (∼2.14 Å (XRD)) (Table 1) and fitted Cu−O_L distance increases (2.16(2) Å (R_{xaf} = 15.1%) and 2.22(2) Å (R_{xaf} = 15.8%)) for [Cu_2(Indo)$_4$(DMF)$_2$] and [Cu_2(Indo)$_4$(OH_2)$_2$], respectively, to 2.17(2) Å (R_{xaf} = 10.9%) and 2.24(2) Å (R_{xaf} = 12.0%)) (Table S6). The weighting (w) of the restraints to XAFS was, therefore, set at w = 1 unless otherwise stated. No significant changes were found in the refined XAFS parameters, bond distances, and bond angles of [Cu_2(Indo)$_4$(DMF)$_2$] (10 K) as a result of the exclusion of the atomic XAFS (AXAFS) region (r < 0.7 Å) other than an improvement in the goodness-of-fit parameter (R_{xafs}) (Table S6). Therefore, all MS refinements used an r window in the Fourier filter of 0.7−4.6 Å.

The MS model excluded contributions from the axial solvent ligand, other than Cu−O_L, unless otherwise stated. In general, the MS model resulted in ∼65 unique MS pathways, where the total distance traveled by the photoelectron (R_{eff}) was less than or equal to 10.0 Å and included no more than 5 legs (n = 5).

The degree of determinacy of the fit (N_i/N_p)[35] was calculated from the number of independent data points (N_i) and parameters (N_p) of the XAFS data set and model, respectively:[35]

$$N_i = \frac{2(\Delta r)(\Delta k)}{\pi} + \sum_i D(N-2) + 1 \quad (2)$$

where Δr and Δk are the ranges of the FT and XAFS filtered data, respectively, and D and N are the number of dimensions (1 for a single degree of freedom, 2 for planar groups) and independent atoms per refinement unit, respectively. The centrosymmetric MS model used in this work, with typical values of Δr and Δk of 3.9 Å and 12.4 Å^{-1}, respectively, gave N_p = 15 (E_o, S_o^2, six positional parameters, and seven Debye−Waller thermal parameters) and has a determinacy of about 2.38, which is well overdetermined.[35]

Where appropriate, the bond distances and angle restraints used for the axial ligand atoms are given in the Supporting Information (Tables S7−S10). The starting positional parameters for the disordered methyl and amide carbon atoms, and the nitrogen atom of the axial DMF ligand were taken from the crystal structure of [Cu_2(Indo)$_4$(DMF)$_2$]·1.6DMF, i.e., C_{41} (occupancy N = 0.48), C_{41}' (N = 0.52), C_{42} (N = 0.38), C_{42}' (N = 0.62), N_3 (N = 1).[17] The bond distance and angle restraints for OH_2 were taken from literature values.[41] The restraints for NMP were taken from the XRD data of a Zn(II) dimer of IndoH,[42] while those for DMA were taken from XRD data of [Cu_2(Indo)$_4$(DMA)$_2$].[43]

(33) Ellis, P. J.; Freeman, H. C. *J. Synchrotron Radiat.* **1995**, *2*, 190−195.
(34) Ellis, P. J. Ph.D. Thesis, University of Sydney, Sydney, Australia, 1995.
(35) Binsted, N.; Strange, R. W.; Hasnain, S. S. *Biochemistry* **1992**, *31*, 12117−12125.
(36) Mustre de Leon, J.; Rehr, J. J.; Zabinsky, S. I.; Albers, R. C. *Phys. Rev. B* **1991**, *44*, 4146−4156.
(37) Rehr, J. J.; Mustre de Leon, J.; Zabinsky, S. I.; Albers, R. C. *J. Am. Chem. Soc.* **1991**, *113*, 5135−5140.
(38) Rehr, J. J.; Albers, R. C. *Phys. Rev. B* **1990**, *41*, 8139−8149.
(39) Ellis, P. J. *XFIT Software*, version 1.1 for WIN 32; ANSTO: Sydney, Australia, 1995.
(40) Rich, A. M. Ph.D. Thesis, University of Sydney, Sydney, Australia, 1997.
(41) Kieninger, M.; Suhai, S. *Int. J. Quantum Chem.* **1994**, *52*, 465−478.
(42) Zhou, Q.; Hambley, T. W.; Kennedy, B. J.; Lay, P. A.; Turner, P.; Warwick, B.; Biffin, J. R.; Regtop, H. L. *Inorg. Chem.* **2000**, *39*, 3742−3748.
(43) Turner, P. Personal communication (University of Sydney), 2000.

Table 1. Comparison between XRD and MS XAFS Data, Including MS XAFS Refined Bond Distances (Å), Debye−Waller Factors (σ^2 (Å^2)), and Bridging O−C−O Bond Angles (deg) of $[Cu_2(Indo)_4L_2]$ (L = DMF, NMP, DMA, OH_2) at RT and 10 K[a]

		bond distance (Å)			bond angle (deg)	Debye−Waller factor (σ^2(Å^2))			XAFS parameter		
complex	temp (K)	Cu···Cu	Cu−O_{Ac}	Cu−O_L	O−C−O	Cu···Cu	Cu−O_{Ac}	Cu−O_L	E_o [b] (eV)	S_o^2 [c]	R_{xaf} (%)
$[Cu_2(Indo)_4(DMF)_2]$	10	2.63(2)	1.96(2)	2.16(2)	125(1)	0.003	0.003	0.004	−8.3	0.91	15.1
$[Cu_2(Indo)_4(DMF)_2]$	RT	2.62(2)	1.95(2)	2.15(2)	125(1)	0.006	0.001	0.01	−9.3	0.91	11.9
$[Cu_2(Indo)_4(DMA)_2]$	10	2.63(2)	1.95(2)	2.12(2)	125(1)	0.003	0.004	0.013	−9.5	0.91	14.1
$[Cu_2(Indo)_4(DMA)_2]$	RT	2.63(2)	1.95(2)	2.11(2)	125(1)	0.007	0.007	0.015	−10.0	0.91	13.4
$[Cu_2(Indo)_4(OH_2)_2]$[d]	10	2.62(2)	1.95(2)	2.19(2)	125(1)	0.003	0.005	0.013	−8.6	0.92	15.1
$[Cu_2(OAc)_4(OH_2)_2]$[d]	10	2.62(2)	1.96(2)	2.14(2)	125(1)	0.004	0.006	0.005	−7.6	0.90	13.3
$[Cu_2(Indo)_4(NMP)_2]$[e−g]	10	2.63(2)	1.95(2)	2.15(2)	125(1)	0.003	0.004	0.010	−9.3	0.93	14.1
$[Cu_2(Indo)_4(NMP)_2]$[e−g]	RT	2.63(2)	1.96(2)	2.15(2)	125(1)	0.007	0.005	0.013	−9.5	0.92	15.5

XRD

complex	temp (K)	Cu···Cu	Cu−O_{Ac}	Cu−O_L	O−C−O (deg)
$[Cu_2(OAc)_4(OH_2)_2]$[h]	RT	2.616(1)	1.969	2.156(4)	124.8(8)
$[Cu_2(Indo)_4(DMF)_2]$[i]	RT	2.630(1)	1.959	2.143(5)	123.9(6)
$[Cu_2(Indo)_4(DMSO)_2]$[j]	RT	2.632(6)	1.95	2.16(2)	NA
$[Cu_2(Indo)_4(DMA)_2]$[k]	RT	2.649(3)	1.96	2.132(6)	125.3(8)
$[Cu_2(Sup)_4(DMF)_2]$[l]	RT	2.641(2)	1.95	2.182(7)	126.6(2)

[a] Cu−O_L starting distance is 2.14 Å and determinacy (N_i/N_p) of the centrosymmetric model is ∼2.2 unless otherwise stated. [b] E_o is relative to the conventional energy edge of 8980.3 eV.[32] [c] S_o^2 is the amplitude reduction factor. [d] Removal of the centrosymmetric restraints $x_0 = -x_1$ and $x_{14} = -x_{15}$, Cu−O_L starting distance 2.14 Å; determinacy (N_i/N_p) = 1.68. [e] Inclusion of NMP atoms. [f] Exclusion of the NMP atoms $[Cu_2(Indo)_4(NMP)_2]$ (RT) (Cu···Cu, 2.63(2) Å (σ^2 = 0.006 Å^2); Cu−O_{Ac}, 1.95(2) Å (σ^2 = 0.006 Å^2); Cu−O_L, 2.11(2) Å (σ^2 = 0.014 Å^2); O−C−O, 125(1)°; E_o = −10.1 eV; S_o^2 = 0.91; R_{xaf} = 14.4%. $[Cu_2(Indo)_4(NMP)_2]$ (10 K) (Cu···Cu, 2.63(2) Å (σ^2 = 0.003 Å^2)); Cu−O_{Ac}, 1.95(2) Å (σ^2 = 0.004 Å^2); Cu−O_L, 2.14(2) Å (σ^2 = 0.012 Å^2); O−C−O, 125(1)°; E_o = −9.6 eV; S_o^2 = 0.92; R_{xaf} = 12.6%). [g] Determinacy (N_i/N_p) = 1.11. [h] Reference 24. [i] Reference 17. [j] Reference 16. [k] Reference 43. [l] Reference 54. The symmetery relationships for the centrosymmetric and noncentrosymmetric MS XAFS models and typical paths and importance factors using the centrosymmetric MS model are given in Tables S4 and S5.

To reduce the refinement time for each MS calculation, curve-wave (CW) and plane-wave (PW) filters were set to 3% and 2%, respectively. Removal of the filters did not affect the value of the refined XAFS parameters (Table S6). Of the additional ∼42 MS pathways added to the ∼65 unique-MS-pathway model (Table S5) on increasing the maximum number of legs from 5 to 6 and removal of CW and PW filters, only three paths (Table S11 of Supporting Information) had importance factors greater than 2% relative to the strongest backscattering path ($Cu_0 \rightarrow O_5 \rightarrow Cu_0$) (Table S5).

Results

TGA. Thermogravimetric analyses of the aqua complexes confirmed about four water molecules per $[Cu_2(Indo)_4(OH_2)_2]$ were absorbed upon storage.[44] Results of the TGA analysis of the aqua complexes, along with plots of the thermogram and proposed stoichiometry for the five-step decomposition profile, are given in the Supporting Information (Figure S2 and Table S12).

XANES. The XAFS and X-ray absorption near-edge spectra (XANES) of all the complexes are similar and, therefore, indicative of a comparable geometry around the Cu absorber. A typical plot is shown in Figure 2 ($[Cu_2(Indo)_4(DMF)_2]$ (10 K)), illustrating the normalized X-ray absorption Cu K-edges, with an inset plot of the weak symmetry-forbidden 1s → 3d preedge transition.

SS Analysis of XAFS Data. The two- and three-shell SS analyses of the XAFS confirm that $[Cu_2(OAc)_4(OH_2)_2]$ (10 K) and $[Cu_2(Indo)_4L_2]$ (L = DMF, NMP, DMA, OH_2) (RT and 10 K) have similar six-coordinate dinuclear structures, with Cu···Cu separations of ∼2.61(2) Å (Tables S13 and S14 of Supporting Information). At 10 K compared to RT, there is a decrease in the value of the Debye−Waller parameters but an increase in the value of the goodness-of-fit parameters R_{xaf} (due to decreased signal-to-noise as a result of X-ray absorption by the cryostat).

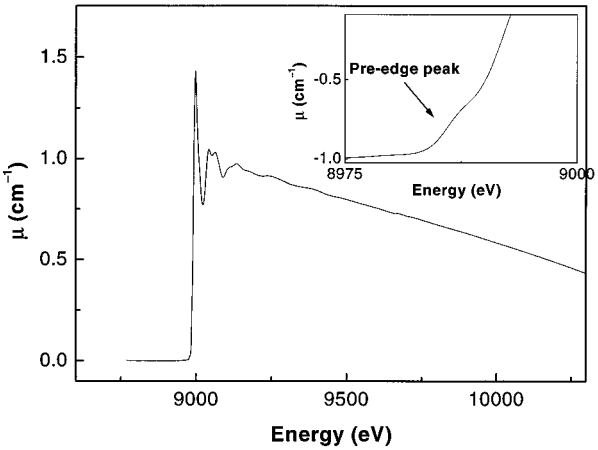

Figure 2. Plots of the normalized X-ray absorption Cu-edge, featureless preedge absorbance, X-ray absorption near-edge, and XAFS oscillations for $[Cu_2(Indo)_4(DMF)_2]$ (10 K). The inset shows the preedge peak.

These Cu···Cu distances are in excellent agreement with those obtained from RT crystallographic studies (2.616(1) Å for $[Cu_2(OAc)_4(OH_2)_2]$,[24] 2.630(1) Å for $[Cu_2(Indo)_4(DMF)_2]$)[17] and are comparable to those obtained from ethanol solution and glass XAS (SS analysis) of $[Cu_2(OAc)_4(OH_2)_2]$ (2.58 Å; σ^2 = 0.08 Å^2 − 2.61 Å; σ^2 = 0.06 Å^2) despite the greater value in the Debye−Waller factor compared to the current work (Tables S13 and S14) indicating a less well-defined Cu···Cu distance.[31,45] The fitted three-shell SS axial Cu−O_L bond length of ∼2.24(2) Å (σ^2 = 0.005 Å^2) for $[Cu_2(OAc)_4(OH_2)_2]$ and $[Cu_2(Indo)_4L_2]$ (L = DMF, DMA, NMP, OH_2) is longer than those in the XRD structures of $[Cu_2(OAc)_4(OH_2)_2]$ (2.156(4) Å)[24] and $[Cu_2(Indo)_4(DMF)_2]$ (2.143(5) Å),[17] despite the resolution of the SS data, i.e., ΔR = 0.12 Å,[29] permitting the differentiation of the axial Cu−O_L bond length from the in-plane Cu−O_{Ac} bond length.

(44) Weder, J. E. Ph.D. Thesis, University of Sydney, Sydney, Australia, 2000. Microanalysis obtained immediately after the preparation of $[Cu_2(Indo)_4L_2]$ (L = OH_2) confirmed less than two water molecules of crystallization per $[Cu_2(Indo)_4(OH_2)_2]$.

(45) Details of the model including the values of the Debye−Waller restraints and standard deviations in the SS-refined distances from the solution XAS of $[Cu_2(OAc)_4(OH_2)_2]$ were not reported.

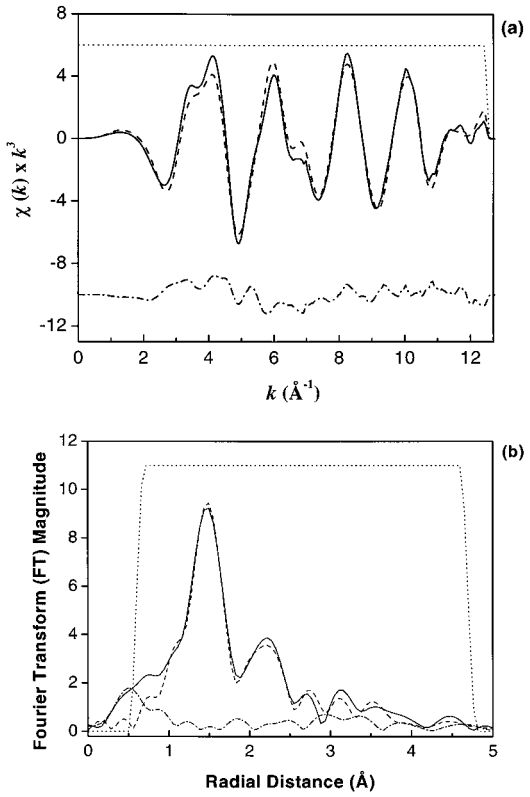

Figure 3. (a) Cu K-edge MS XAFS data observed (−), simulated (- - -), and residual (-•-) for $[Cu_2(Indo)_4(DMA)_2]$ at 10 K (R_{xaf} = 14.1%). The region shown by (•••) is the *k* window used in the Fourier filter. (b) Corresponding MS Fourier transform observed (−), simulated (- - -), and residual (-•-) of the XAFS data from the XAFS spectrum of $[Cu_2(Indo)_4(DMA)_2]$ at 10 K. The region shown by (•••) is the *r* window used in the Fourier filter.

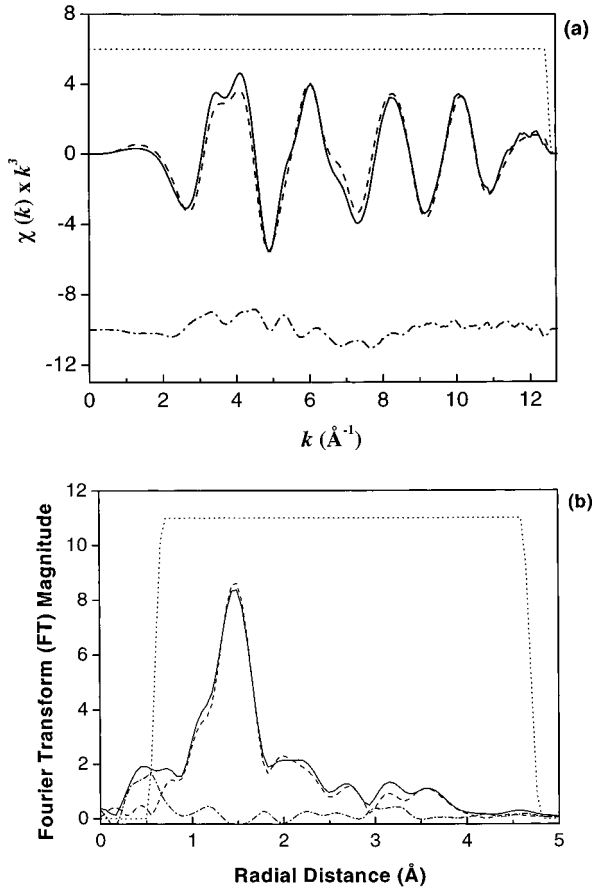

Figure 4. (a) Cu K-edge MS XAFS data observed (−), simulated (- - -), and residual (-•-) for $[Cu_2(Indo)_4(DMF)_2]$ at RT (R_{xaf} = 11.9%). The region shown by (•••) is the *k* window used in the Fourier filter. (b) Corresponding MS Fourier transform observed (−), simulated (- - -), and residual (-•-) of the XAFS data from the XAFS spectrum of $[Cu_2(Indo)_4(DMF)_2]$ at RT. The region shown by (•••) is the *r* window used in the Fourier filter.

The refined three-shell SS-derived Cu−O_L bond is similar to that reported from the XAS of $[Cu_2(OAc)_4(OH_2)_2]$ in a vitrified aqueous glycerol sample (Cu−O_L = 2.28 Å (σ^2 = 0.07 Å^2)) and ethanol sample at RT (Cu−O_L = 2.37 Å (σ^2 = 0.13 Å^2), ∼60% Cu(II) dimer content).[31] However, a glassy ethanol sample (of unknown Cu(II) dimer content) has a reported Cu−O_L distance of 2.12 Å (σ^2 = 0.05 Å^2).[31]

The R_{xaf} value for the seven-shell SS model was unacceptable, i.e., 30.9%. The (unrestrained) seven-shell SS analysis of $[Cu_2(Indo)_4(DMF)_2]$ (10 K) gave a dinuclear Cu···Cu separation of 2.64(2) Å, Cu−O_{Ac} of 1.96(2) Å (for N = 2, 5, 7, 8) and 3.14 Å (for N = 3, 4, 6, 9), and Cu···C of 2.87(2) Å (for N = 10, 11, 12, 13) (Table S3). Distance restraints from Cu_0 to the axial oxygen atoms (N = 14, 15) of 2.14(2) and 4.77(2) Å, respectively, and β-carbon atoms (N = 20, 21, 22, 23) of 4.24(2) Å (R_{xaf} = 39.5%) (Figure S3) were required to model these distances to within experimental error of the XRD distances of $[Cu_2(Indo)_4(DMF)_2]$·1.6DMF.[17]

MS Fitting of XAFS Data. The MS-fitted bond distances and Debye−Waller factors for the Cu···Cu vector length, mean Cu−O_{Ac} and axial Cu−O_L bond distances, and bridging O−C−O bond angle for $[Cu_2(OAc)_4(OH_2)_2]$ and $[Cu_2(Indo)_4L_2]$ (L = DMF, DMA, NMP, OH_2) at RT and 10 K are given in Table 1. The paths and importance factors using the centrosymmetric MS model for the MS refinement of the XAFS of $[Cu_2(Indo)_4(DMF)_2]$ (10 K) are given in Table S5. The fits of the XAFS for $[Cu_2(Indo)_4(DMA)_2]$ at 10 K (R_{xaf} = 14.1%) and $[Cu_2(Indo)_4(DMF)_2]$ at RT (R_{xaf} = 11.9%) and corresponding Fourier transforms are shown in Figures 3 and 4, respectively. The fits of the XAFS and corresponding Fourier transform for $[Cu_2(OAc)_4(OH_2)_2]$ (10 K), using the noncentrosymmetric model without symmetry restraints on the Cu and axial oxygen ligands along the *x* axis (R_{xaf} = 13.3%), is given in Figure 5. Fits of the XAFS of $[Cu_2(Indo)_4L_2]$ (L = NMP, OH_2) at 10 K and the corresponding Fourier transforms using the centrosymmetric MS model are given in the Supporting Information (Figures S4 and S5).

The MS fit resulted in Cu···Cu, Cu−O_L, and mean Cu−O_{Ac} bond lengths of 2.63(2), 2.16(2), and 1.96(2) Å, respectively, for $[Cu_2(Indo)_4(DMF)_2]$ at 10 K (R_{xaf} = 15.1%, N_i/N_p = 2.27), which are in excellent agreement with the crystallographic values (Table 1)[17] and those for $[Cu_2(Indo)_4(DMSO)_2]$ (Table 1).[16] The refined Cu···Cu, Cu−O_L, and mean Cu−O_{Ac} bond lengths of 2.63(2), 1.95(2), and ∼2.13(2) Å, respectively, for $[Cu_2(Indo)_4L_2]$ (L = DMA, NMP) at RT and 10 K and $[Cu_2(Indo)_4(DMF)_2]$ at RT are similar to those of $[Cu_2(Indo)_4(DMF)_2]$ at 10 K. There are slight decreases in the values of the Debye−Waller parameters and an increase in the values of the goodness-of-fit parameters at 10 K compared to RT.

The fitted bond distances of the $Cu_2O_{10}C_8$ dimer core were unchanged because of the inclusion of the C and N atoms of the DMF ligands (Tables S15 and S16 of Supporting Information). The incorporation into the ∼65-unique-MS-pathway model (Table S5) of these additional axial DMF atoms and the removal of CW and PW filters results in a ∼263-unique-MS-pathway model. Of the further ∼198 unique MS pathways incorporated into the centrosymmetric model as a result of the

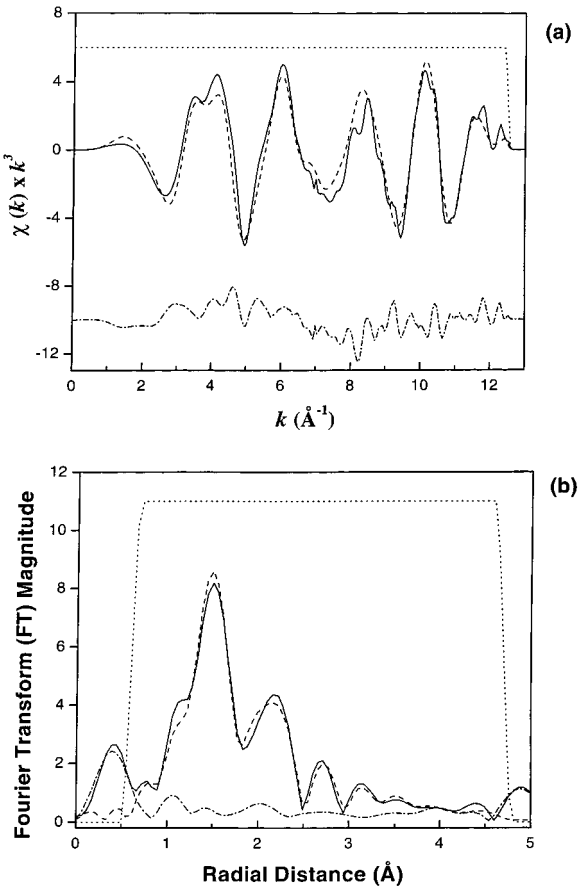

Figure 5. (a) Cu K-edge MS XAFS data observed (−), simulated (- - -), and residual (-•-) for $[Cu_2(OAc)_4(OH_2)_2]$ at 10 K (R_{xaf} = 13.3 %) using the noncentrosymmetric MS model. The region shown by (•••) is the *k* window used in the Fourier filter. (b) Corresponding MS Fourier transform observed (−), simulated (- - -), and residual (-•-) of the XAFS data from the XAFS spectrum for $[Cu_2(OAc)_4(OH_2)_2]$ at 10 K using the noncentrosymmetric model. The region shown by (•••) is the *r* window used in the Fourier filter.

inclusion of these DMF ligand atoms, only six MS pathways had importance factors relative to the strongest backscattering path, i.e., $Cu_0 \rightarrow O_5 \rightarrow Cu_0$, greater than 2% (Table S17 of Supporting Information). While the MS-fitted values of the Debye−Waller parameters for the nitrogen atom (σ^2 = 0.01 Å^2) and the disordered amide carbon atom (C_{41}) (σ^2 = 0.03 Å^2) are acceptable (Table S15), the values for the remaining DMF ligand atoms approached their restraints (Table S16), indicating that they do not make significant contributions.

The fitted Cu−O_L distance decreased from an expected 2.132(6) Å[43] (Table 1) to ∼2.00(2) Å (R_{xaf} = 15.0%, N_i/N_p = 1.68) upon inclusion of the C and N atoms of the DMA ligand into the centrosymmetric MS model for the XAFS of $[Cu_2(Indo)_4(DMA)_2]$ (10 K). The fitted bond distances, bond angles, and Debye−Waller factors are given in Table S18 of Supporting Information. For $[Cu_2(Indo)_4(NMP)_2]$, inclusion of the C and N atoms of the more rigid NMP ligand resulted in a fitted Cu−O_L distance of 2.15(2) Å (R_{xaf} = 15.5%, N_i/N_p = 1.11) (Table S19 of Supporting Information) compared to 2.11(2) Å (R_{xaf} = 13.4%, $N_i/N_p \approx$ 2.2) without including the NMP (Table 1). These fitted Cu−O_L distances for $[Cu_2(Indo)_4(NMP)_2]$ are, however, within experimental error.

The fitted Cu•••Cu and mean Cu−O_{Ac} bond lengths of 2.63(2) and 1.95 Å, respectively, for $[Cu_2(OAc)_4(OH_2)_2]$ (10 K) and $[Cu_2(Indo)_4(OH_2)_2]$ (RT and 10 K) are similar to those for $[Cu_2(Indo)_4L_2]$ (L = DMA, NMP, DMF) and the XRD values for $[Cu_2(OAc)_4(OH_2)_2]$,[24] $[Cu_2(Indo)_4(DMF)_2]$,[17] and $[Cu_2(Indo)_4(DMSO)_2]$[16] (Table 1). However, the fitted Cu•••O_L bond lengths for $[Cu_2(OAc)_4(OH_2)_2]$ (10 K) and $[Cu_2(Indo)_4(OH_2)_2]$ (10 K and RT) of ∼2.21(2) Å (Table S6) are longer than expected from crystallographic data ($[Cu_2(OAc)_4(OH_2)_2]$ = 2.156(4) Å)[24] and $[Cu_2(Indo)_4(DMF_2)_2]$ = 2.143(5) Å)).[17] These long Cu−$O_{(OH_2)}$ bond lengths were obtained from the fit irrespective of the value of the starting Cu•••O_L bond length, inclusion or exclusion of CW and PW filters, increase in the value of the weight of the restraints to XAFS from 1 to 8, increase in the effective MS path length (R_{eff}) from 10.0 to 10.2 Å, the synthetic route for the preparation of $[Cu_2(Indo)_4(OH_2)_2]$, or an increase in the maximum number of legs per MS pathway from five to six (Table S6).

The removal of symmetry restraints along the *x* axis for the copper and axial oxygen atoms from the centrosymmetric MS model (N_i/N_p = 1.68) results in an excellent fit for the Cu−$O_{(OH_2)}$ bond distances of 2.14(2) Å for $[Cu_2(OAc)_4(OH_2)_2]$ (Table 1). The corresponding value for $[Cu_2(Indo)_4(OH_2)_2]$ (2.19(2) Å) (Table 1) is within experimental error of that derived from the XRD data for $[Cu_2(Indo)_4(DMSO)_2]$ of 2.16(2) Å.[16] The removal of all symmetry restraints on the carboxylate cages of the centrosymmetric MS model results in an underdetermined model ($N_i/N_p \approx$ 0.7) and, therefore, was not investigated.

The fitted bridging O−C−O bond angles of 125(1)° for $[Cu_2(Indo)_4L_2]$ (L = DMF, DMA, NMP) (Table 1) are independent of the axial ligand and in excellent agreement with XRD values for $[Cu_2(Indo)_4(DMF)_2]$ (123.9(6)°)[17] and $[Cu_2(OAc)_4(OH_2)_2]$ (124.8(8)°).[24] Furthermore, the Cu−O−C−O−Cu bridge lengths (∼6.42 Å), sum of the Cu−O bond lengths around the Cu core (including the half Cu•••Cu distance, ∼11.27 Å), and displacement of the Cu atom out of the Cu−O_{Ac} plane (∼0.20 Å) for $[Cu_2(Indo)_4L_2]$ (L = DMF, DMA, NMP) (Table S20 of Supporting Information) are similar to values reported elsewhere for related dimeric Cu(II) carboxylate compounds.[46−48]

Discussion

Comparison of SS Fits with MS Fits. The use of MS fitting of XAFS data for the dinuclear Cu complexes demonstrates for the first time the ability of the technique to reproduce accurately the bonding about the Cu sites, where SS analysis has been unsuccessful (at least for the axial ligands).[31] The problem of SS analysis being unable to reproduce axial Cu−O_L bond lengths has been further highlighted here in the two-, three-, and seven-shell SS models. By contrast, the agreements of the refined bond distances, the bridging O−C−O angle, and the displacement of the Cu out of the plane of the XAFS of $[Cu_2(Indo)_4(DMF)_2]$ with crystallographic data are excellent using MS analyses and show the power of this technique for obtaining accurate angular and bond length information about the Cu atom. Together with the low values of R_{xaf}, these confirm the validity of centrosymmetric MS XAFS analysis to determine the structures of other complexes of pharmaceutical interest for which suitable crystals for XRD have yet to be obtained/reported ($[Cu_2(Indo)_4L_2]$ (L = DMA, NMP, OH_2)). Thus, the ability to provide accurate and precise MS fits in such complexes is an important contribution to extending their veterinary and human pharmaceutical applications because such complexes need to be characterized before they can be registered. The $[Cu_2(Indo)_4L_2]$ complexes have a coordination and geometry similar

(46) Sundberg, M. R.; Uggla, R.; Melnik, M. *Polyhedron* **1996**, *15*, 1157−1163.
(47) Melnik, M. *Coord. Chem. Rev.* **1981**, *36*, 1−44.
(48) Melnik, M. *Coord. Chem. Rev.* **1982**, *42*, 259−293.

to those reported for other Cu(II) acetate type dimers containing a $Cu_2O_{10}C_8$ core.[46,48−50] Such results are consistent with the comparable magnetic and spectroscopic data obtained for all of the complexes.[17]

While the two- and three-shell SS analyses confirm similar dimeric coordination for $[Cu_2(OAc)_4(OH_2)_2]$ and $[Cu_2(Indo)_4L_2]$ (L = DMF, NMP, DMA, OH_2), the refined (three-shell) Cu−O_L bond distance of ∼2.24 Å is ∼0.1 Å longer than those determined from XRD data.[16,17,24] This is despite the resolution of the data permitting the differentiation of the axial Cu−O_L from the in-plane Cu−O_{Ac} bond length.[29] The inclusion of additional SS shells, e.g., seven shells, improves the fitting of the XAFS data for $[Cu_2(Indo)_4(DMF)_2]$ but not the refined axial bond lengths. The limitation of the seven-shell SS model is also highlighted by its inability to satisfactorily reproduce the XRD-determined Cu···C and Cu−O_L distances. The large residual, particularly for *r* greater than 3 Å, and unacceptably high value (R_{xaf} = 30−40%) highlights the need to include backscattering contributions from unmodeled MS pathways.

Strong hydrogen bonding occurs in crystalline $[Cu_2(OAc)_4(OH_2)_2]$, with each dimer being linked by eight hydrogen bonds to four neighboring molecules.[23,24] As a result, an elongation by ∼0.04 Å occurs for Cu−O_{Ac} bonds hydrogen-bonded via the axial aqua ligand to oxygen acceptor atoms in a neighboring dimer, relative to the Cu−O_{Ac} bonds not involved in hydrogen bonding. The distances of the Cu absorber to the oxygen acceptor atoms of a neighboring $[Cu_2(OAc)_4(OH_2)_2]$ dimer is 4.818(1) and 4.219(2) Å].[24] Inclusion of oxygen acceptor atoms of a neighboring $[Cu_2(OAc)_4(OH_2)_2]$ dimer into the MS model did not change the fitted Cu−$O_{(OH_2)}$ bond length (2.22 Å) (Table S6). The inability of the centrosymmetric MS model to accommodate elongation of the Cu−O_{Ac} bonds arising from hydrogen bonding to a neighboring dimer may contribute to the difficulties in reproducing the XRD-observed Cu−$O_{(OH_2)}$ distances in $[Cu_2(OAc)_4(OH_2)_2]$. Since the structure of $[Cu_2(OAc)_4(OH_2)_2]$ is similar at 183 and 293 K,[24,51] it is unlikely that the geometry of $[Cu_2(OAc)_4(OH_2)_2]$ at 10 K is sufficiently different to result in a significant change in the Cu−$O_{(OH_2)}$ distance. There is, however, isotropic contraction by 0.3−0.4% along all of the axes at 183 K compared to results at 293 K.[51] The excellent fit to the Cu−$O_{(OH_2)}$ distance of $[Cu_2(OAc)_4(OH_2)_2]$ (mean Cu−O_L distance of 2.14(2) Å, R_{xaf} = 13.3%) using the lower symmetry model is consistent with the greater distortions from a centrosymmetric model in the XRD structure.[24] While this model had more adjustable parameters, the fit was still overdetermined (N_i/N_p = 1.68).[35] A similar lowering of the symmetry of the Cu−O_{Ac} bonding around Cu_0 may also occur because of hydrogen bonding in $[Cu_2(Indo)_4(OH_2)_2]\cdot nH_2O$. This is consistent with the need to use the lower symmetry MS model to obtain a value for the Cu−$O_{(OH_2)}$ bond length from the $[Cu_2(Indo)_4(OH_2)_2]$ XAFS data similar to that from $[Cu_2(Indo)_4(DMSO)_2]$ (2.16 Å (XRD)).[16] Such a Cu−$O_{(OH_2)}$ bond length is consistent with the similarity in both the Cu···Cu distances and the magnetic coupling in the series of complexes.[17] The distortion and intercomplex interactions implied by MS fitting to the XAFS were previously proposed to explain the somewhat different magnetic behavior of $[Cu_2(Indo)_4(OH_2)_2]\cdot nH_2O$ at very low temperatures compared to the other Indo complexes.[17]

Contributions of Outer Ligand Atoms and Intermolecular Contacts. Studies of aqueous solution (SS XAFS) of $Cu(NO_3)_2$ and $Cu(ClO_4)_2$ revealed backscattering contributions from a second hydration shell at ∼4 Å from the absorbing Cu(II) center.[52,53] The inclusion into the centrosymmetric MS model of a second hydration shell around the axial aqua ligand of $[Cu_2(Indo)_4(OH_2)_2]$ did not result in any significant changes in the refined XAFS parameters or in the Cu−O_L bond distance of 2.22 Å (Table S6).

The inability to fit the positional parameters for all the DMF ligand atoms in $[Cu_2(Indo)_4(DMF)_2]$ is not surprising given their disorder.[17] MS fitting that incorporated backscattering contributions from the pendent Indo groups (crystal structure atoms C3, C23, and C9a at ∼2.47 Å from Cu_0) and neighboring dimer molecules (crystal structure atoms C34x and C43x at ∼4.18 Å from Cu_0) of $[Cu_2(Indo)_4(DMF)_2]$ indicated highly disordered positional parameters for these atoms, as evidenced by large errors in the refined positional parameters. This is consistent with the low symmetry of the IndoH moieties in the crystal structure (Table S2). As a consequence, only the $Cu_2O_{10}C_8$ model of the dimer core, including the α and β carbon atoms (*N* = 20, 21, 22, 23) of the carboxylate of the Indo groups, was used in the MS analyses of the XAFS data of $[Cu_2(Indo)_4L_2]$ (L = DMA, NMP), unless otherwise stated. Because scattering is reliably observed from atoms 4−5 Å from the metal absorber,[29] the current work excludes scattering contribution from atoms at a distance greater than 5.0 Å from the Cu atom in the NMP ligand.

The fitted Cu−O_L distance of 2.15(2) Å (R_{xaf} = 15.5% (10 K)) when all the atoms of the NMP ligand within 5 Å of Cu_0 are included in the model for $[Cu_2(Indo)_4(NMP)_2]$ is closer to that derived from the XRD data for $[Cu_2(Indo)_4(DMF)_2]$ (2.143(5) Å), compared to the MS fit that excludes these ligand atoms (2.11(2) Å (R_{xaf} = 14.4% (10 K)) (Table 1). The restrained and rigid nature of the NMP ligand increases MS contributions and may explain its successful inclusion in the MS model compared to the disordered DMA and DMF adducts.

The unmodeled scattering contributions for *r* greater than 3.0 Å are probably due to the unmodeled atoms in the axial ligands, Indo moieties, neighboring dimer units, and unligated solvent molecules. This observation is supported by the slightly different residual FT spectra observed in this range for different axial ligands. However, these contributions are unimportant in reproducing XRD data for the $Cu_2O_{10}C_8$ core.[17]

Relationship between Structural Data and Physical Properties. Several reviews of the relationship between structural data and physical properties in dimeric Cu(II) carboxylate complexes have been published[46−49] and demonstrate a limited range (∼0.02 Å) of bond distances in some structural parameters for CuO_4O or CuO_4N chromophores.[46−48,54] The comparable empirical parameters determined from the analyses of the XAFS data of $[Cu_2(Indo)_4L_2]$ (L = DMF, DMA, NMP) fall within the expected range for CuO_4O chromophores[46−48] (Table S20).

An increase in the Cu···Cu separation with increasing acid strength of the bridging carboxylate group of Cu(II) dimers has

(49) Doedens, R. J. *Prog. Inorg. Chem.* **1976**, *21*, 209−231.
(50) Catterick, J.; Thornton, P. *Adv. Inorg. Chem. Radiochem.* **1977**, *20*, 291−362.
(51) Shamuratov, E. B.; Batsanov, A. S.; Shapirov, Kh. T.; Struchkov, Yu. T.; Azizov, T. *Russ. J. Coord. Chem. (Engl. Transl.)* **1994**, *20*, 710−711.
(52) Licheri, G.; Musinu, G.; Paschina, G.; Piccaluga, G.; Pinna, G.; Sedda, A. F. *J. Chem. Phys.* **1984**, *80*, 5308−5311.
(53) Magini, M. *Inorg. Chem.* **1982**, *21*, 1535−1538.
(54) The Cu(II) complex of the NSAID Suprofen = SupH ($[Cu_2(Sup)_4(CH_3CN)_2]$) (a CuO_4N chromophore) gives an interatomic distance around the Cu atom (including the half value of the Cu···Cu distance) of 11.318(29) Å and Cu−OAc distances of 1.955(5) and 1.933(5) Å). This does not fit the empirical relationships.[46−48] Details of the XRD of $[Cu_2(Sup)_4(CH_3CN)_2]$ are taken from the following. Kögerler, P.; Williams, P. A. M.; Parajón-Costa, B. S.; Baran, E. J.; Lezama, L.; Rojo, T.; Müller, A. *Inorg. Chim. Acta* **1998**, *268*, 239−248.

been reported.[46−49] The most significant structural change accompanying this increase in the Cu···Cu separation is the movement of the Cu atom out of the basal plane of the square pyramid. The similar Cu···Cu distances for $[Cu_2(Indo)_4L_2]$ (L = DMF, DMA, NMP, OH_2) are marginally longer than that for $[Cu_2(OAc)_2(OH_2)_2]$ of 2.616(1) Å (XRD)[24] and 2.61(2) Å (XAFS). The slightly longer Cu···Cu separation for $[Cu_2(Indo)_4(DMF)_2]$ is consistent with a slightly greater IndoH acidity ($pK_a = 4.5$)[55] compared to that of acetic acid ($pK_a = 4.8$)[55] and with a correspondingly greater displacement of the Cu atom from the basal plane of 0.20 Å for $[Cu_2(Indo)_4(DMF)_2]$ compared to 0.19 Å for $[Cu_2(OAc)_2(OH_2)_2]$.[48] Even though these changes are not significant, the systematic errors are probably constant within the series, and the differences are consistent with the empirical models.

The different behavior of the aqua complex (from the DMF, DMA, and NMP complexes) in fitting with the centrosymmetric model enables it to be distinguished from the other adducts and may be useful in determining aqueous axial ligand exchange of $[Cu_2(Indo)_4(DMF)_2]$ in veterinary pharmaceuticals where water may become an axial ligand.[13]

Conclusions

MS analyses of RT and 10 K XAFS data for $[Cu_2(Indo)_4(DMF)_2]$ reproduces the crystal structure bond lengths and angles for the $Cu_2O_{10}C_8$ core where SS analyses are deficient. Similar MS-refined bond distances and angles were obtained for $[Cu_2(Indo)_4L_2]$ (L = DMF, DMA, NMP). The reduced symmetry around the Cu absorber atom of $[Cu_2(OAc)_4(OH_2)_2]$ and $[Cu_2(Indo)_4(OH_2)_2]$ due to hydrogen bonding of the axial aqua ligand to neighboring dimer units and unligated water molecules requires the removal of symmetry restraints along the Cu axis to fit the $Cu-O_{(OH_2)}$ bond distances observed in the crystal structure of $[Cu_2(OAc)_4(OH_2)_2]$. The MS-fitted geometry of the bidentate carboxylate cage of $[Cu_2(Indo)_4L_2]$ (L = DMF, DMA, NMP, OH_2) and $[Cu_2(OAc)_4(OH_2)_2]$ is consistent with their similar magnetic and spectroscopic data.[17] Further work will include the use of the centrosymmetric MS model to determine the structure of $[Cu_2(Indo)_4(DMF)_2]$ in a variety of veterinary pharmaceutical formulations and to examine for aqua ligand exchange.

(55) *The Merck Index*, 11th ed.; Budavari, S., Ed.; Merck & Co., Inc.: Rahway, NJ, 1989.

Acknowledgment. We acknowledge the support of the Australian Research Council for an SPIRT grant and an RIEFP grant for the 10-element Ge detector. Biochemical Veterinary Research (B.V.R) is gratefully acknowledged for funding, including a postgraduate scholarship for J.E.W., and for helpful discussions with Dr. Ray Biffin and Mr. Barry Warwick on the Cu pharmaceuticals. X-ray absorption spectroscopy was performed at the Australian National Beamline Facility with support from the Australian Synchrotron Research Program, which is funded by the Commonwealth of Australia under the Major National Research Facilities Program. We also thank Dr. James Hester and Dr. Paul Ellis for assistance during the course of the XAFS data collection and analyses, respectively. We also thank Dr. Peter Turner for the calculation of the bond distances of $[Cu_2(OAc)_4(OH_2)_2]$ to neighboring dimers.

Supporting Information Available: Figures of the atomic numbering system for the Indo moieties of $[Cu_2(Indo)_4(DMF)_2]\cdot 1.6DMF$; TGA plots and derivative plots of the thermal decomposition of IndoH, $[Cu_2(Indo)_4(OH_2)_2]\cdot 1.5H_2O$, and $[Cu_2(Indo)_4(OH_2)_2]$; seven-shell SS fits to the Cu K-edge data for $[Cu_2(Indo)_4(DMF)_2]$ at 10 K incorporating restraints and the corresponding Fourier transform; plots of the fits to the Cu K-edge MS XAFS data for $[Cu_2(Indo)_4(NMP)_2]$ at 10 K and $[Cu_2(Indo)_4(OH_2)_2]$ at 10 K and the corresponding fits to their Fourier transforms; fits to the Cu K-edge MS XAFS data for $[Cu_2(OAc)_4(OH_2)_2]$ at 10 K incorporating $Cu-O_{(OH_2)}$ bond length restraints of 2.14(2) Å and the corresponding MS Fourier transform; tables of the Debye−Waller (σ^2 (Å^2)) and positional parameter (x, y, z) constraints, bond angle (deg) and bond length (Å) restraints, and Debye−Waller restraints (σ^2 (Å^2)) in the MS XAFS models; two-, three-, and seven-shell SS-refined bond distances (Å) and Debye−Waller factors (σ^2 (Å^2)) for the Cu···Cu, mean $Cu-O_{Ac}$, and $Cu-O_L$ distances; distance (Å) from XAFS Cu absorber (Cu_0) and positional parameters (x, y, z) of the XAFS model atoms less than 5.5 Å from Cu_0; MS paths and importance factors for the centrosymmetric MS model of $[Cu_2(Indo)_4(DMF)_2]$ (10 K); MS-refined structural data for the bridging groups of $[Cu_2(Indo)_4L_2]$ (L = DMF, DMA, NMP); description and results of additional MS analyses of the XAFS data of $[Cu_2(Indo)_4L_2]$ (L = DMF, DMA, NMP OH_2) and $[Cu_2(OAc)_4(OH_2)_2]$; raw absorbance XAFS data for $[Cu_2(OAc)_4(OH_2)_2]$ and $[Cu_2(Indo)_4L_2]$ (L = DMF, DMA, NMP OH_2) at 10 K; additional MS pathways incorporated into the centrosymmetric model because of the inclusion of the DMF ligand, exclusion of CW and PW filters, increase in the maximum number of legs per MS pathway from five to six, and increase in the distance from Cu_0 to backscattering atom (R_{as}) from 5.0 to 5.1 Å; results of the MS refinements incorporating the NMP and DMA ligands. This material is available free of charge via the Internet at http://pubs.acs.org.

IC0007815